Letter

Heavy-flavor transport and hadronization in pp collisions

Andrea Beraudo,[1,*] Arturo De Pace,[1] Daniel Pablos,[1,2,3] Francesco Prino,[1] Marco Monteno,[1] and Marzia Nardi[1]

[1]*INFN—Sezione di Torino, via Pietro Giuria 1, I-10125 Torino*

[2]*Departamento de Física, Universidad de Oviedo, Avda. Federico García Lorca 18, 33007 Oviedo, Spain*

[3]*Instituto Universitario de Ciencias y Tecnologías Espaciales de Asturias (ICTEA), Calle de la Independencia 13, 33004 Oviedo, Spain*

(Received 12 June 2023; accepted 13 December 2023; published 9 January 2024)

Recent experimental results on the Λ_c^+/D^0 ratio in proton-proton (pp) collisions have revealed a significant enhancement compared to expectations based on universal fragmentation fractions/functions across different colliding systems, from e^+e^- to pp. This unexpected enhancement has sparked speculation about the potential effects of a deconfined medium impacting hadronization, previously considered exclusive to heavy-ion collisions. In this study, we propose a novel approach that assumes the formation of a small, deconfined, and expanding fireball even in pp collisions, where charm quarks can undergo rescattering and hadronization. We make use of the same in-medium hadronization mechanism developed for heavy-ion collisions, which involves local color-neutralization through recombination of charm quarks with nearby opposite color charges from the background fireball. Our model incorporates the presence of diquark excitations in the hot medium, which promotes the formation of charmed baryons. Moreover, the recombination process, involving closely aligned partons from the same fluid cell, effectively transfers the collective flow of the system to the final charmed hadrons. We show that this framework can qualitatively reproduce the observed experimental findings in heavy-flavor particle-yield ratios, p_T-spectra and elliptic-flow coefficients. Our results provide new, complementary supporting evidence that the collective phenomena observed in small systems naturally have the same origin as those observed in heavy-ion collisions.

DOI: 10.1103/PhysRevD.109.L011501

Introduction. Recent heavy-flavor measurements in proton-proton (pp) collisions found a surprisingly large value of the Λ_c^+/D^0 and Ξ_c^0/D^0 ratios [1,2], strongly enhanced with respect to expectations based on fragmentation fractions extracted from e^+e^- data and compatible with results obtained in heavy-ion collisions. Since in this last case the baryon enhancement, primarily observed at intermediate transverse momenta, is commonly attributed to a recombination process between heavy quarks and thermal partons from the hot, deconfined medium generated after the collision, this raises the question of whether a similar mechanism of hadronization can occur in proton-proton collisions, in which a small droplet of quark-gluon-plasma (QGP) might also be produced. This was the idea proposed for instance in Refs. [3,4], which led the authors to satisfactory describe the Λ_c^+/D^0 ratio measured in pp collisions at the LHC. Another attempt to interpret the enhanced production of charmed baryons was based on the statistical hadronization model [5], assuming a thermal population of the different charmed meson and baryon states predicted by the relativistic quark model around a universal hadronization temperature. Reproducing such observations is a challenge for QCD event generators, but recent color-reconnection (CR) models implemented in PYTHIA 8 [6] can provide a satisfactory description of the data, allowing a rearrangement of the confining potential among the partons before hadronization which decreases the energy stored in the color field and favors the production of baryons.

In this paper we propose that the same mechanism of heavy-flavor hadron production at work in heavy-ion collisions occurs in the pp case, assuming that also in proton-proton collisions a small deconfined fireball, with a hydrodynamic expansion driven by pressure gradients, is formed. Such a hot medium affects the stochastic propagation, modeled through a relativistic Langevin equation, of the heavy quarks before hadronization and acts as a reservoir of color charges with which they can undergo recombination when reaching a fluid cell around the hadronization temperature T_H. Both the description of the heavy-quark dynamics through the fireball [7,8] and

*beraudo@to.infn.it

the modelling of their local color-neutralization with opposite-charge thermal particles during hadronization [9] have been described in detail in previous publications. In the following we will give just a brief summary, focusing instead on providing a realistic modelling of the bulk background environment produced in proton-proton collisions. Notice that, going from nucleus-nucleus to proton-proton collisions, we do not fine-tune any parameter of our transport and hadronization models, since our purpose is not to perform a precision-fit of the data, but to show that a consistent description of heavy-flavor production in both systems can be obtained within the same theoretical framework.

Theoretical framework. The entropy deposited at midrapidity by the collision of two nucleons can be constrained by the final-particle multiplicity. It is well-known that many of the observables associated to the emergence of collectivity can be understood assuming that, shortly after the collision, the system behaves hydrodynamically, translating spatial asymmetries of the initial condition into anisotropies of the momentum distributions of the final particles [10,11]. Confrontation with experiments involving small colliding systems (i.e. proton-proton and proton-nucleus) highlighted the role of subnucleonic fluctuations [12]. In order to obtain realistic event-by-event (EBE) initial conditions we use the T$_{\rm R}$ENTo model [13], which simulates the initial entropy deposition by the subnucleonic constituents of the two protons, here assumed to collide at $\sqrt{s} = 5.02$ TeV. This requires setting values for a few parameters, related to the dependence of the deposited entropy on the thickness function of the two incoming protons ($p = 0$, corresponding to a geometric mean, akin to the result obtained from gluon saturation at small x [14]), to the fluctuating weight of each constituent to the process ($k = 0.3$), to the number of subnucleonic constituents ($n_c = 6$) and to the nucleon ($w = 0.92$ fm) and constituent ($v = 0.43$ fm) widths. An overall normalization is also necessary to ensure that at the end of the hydrodynamic evolution one obtains a charged-particle pseudorapidity-density $dN_{\rm ch}/d\eta$ (here coming entirely from soft processes) in agreement with the measured one [15]. At the initial longitudinal proper-time τ_0 the entropy density around space-time rapidity $\eta_s = 0$ is given by

$$s_0(\vec{x}_\perp)|_{\eta_s=0} = \frac{dS_0}{d\vec{x}_\perp dz}\bigg|_{z=0} = \frac{1}{\tau_0}\left(\frac{dS_0}{d\vec{x}_\perp d\eta_s}\right)_{\eta_s=0}, \quad (1)$$

where the quantity in parentheses is the T$_{\rm R}$ENTo output, while $s_0(\vec{x}_\perp)$ (in units of fm^{-3}) is the quantity used to initialize at $\tau_0 = 0.4$ fm/c the subsequent $2+1$ hydrodynamic evolution, evaluated with the MUSIC code [17–19]. Hydrodynamic equations are solved using the equation of state by the Hot-QCD Collaboration [20] and setting a

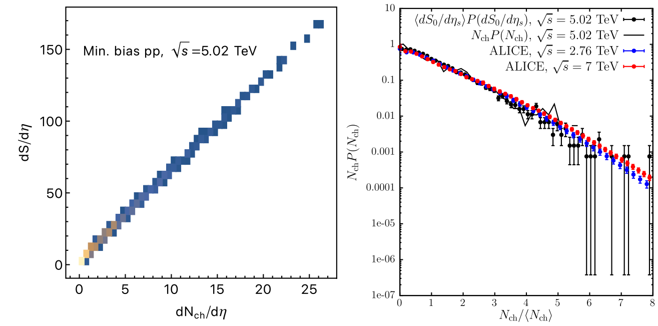

FIG. 1. Left: correlation between the (spacetime/pseudo)rapidity density of initial deposited entropy and final charged particles in our modelling of pp collisions at $\sqrt{s} = 5.02$ TeV. Right: KNO scaling [25] of the charged-particle distribution in pp collisions. Results referring to our initial conditions and hydrodynamic calculations are compared to ALICE data from Ref. [24] for NSD events at $\sqrt{s} = 2.76$ TeV and $\sqrt{s} = 7$ TeV.

constant specific shear viscosity $\eta/s = 0.13$ and nonvanishing bulk-viscosity over entropy-density parameter ζ/s, whose temperature dependence we parametrize as in [21]. The deposited entropy around midrapidity is given by

$$\frac{dS_0}{d\eta_s} = \tau_0 \int d\vec{x}_\perp s_0(\vec{x}_\perp) \quad (2)$$

and is directly related to final charged-particle multiplicity per unit rapidity. From the left panel of Fig. 1 one appreciates the perfect linear correlation between the two quantities, $dS/d\eta_s \sim dN_{\rm ch}/d\eta$, with proportionality coefficient $K \approx 7.2$. Particle distributions are obtained via the Cooper-Frye method [22], particlizing the fluid cells on a isothermal freezeout hypersurface, taking for soft hadrons the decoupling temperature $T_{\rm FO} = 145$ MeV. Our initial conditions, after EBE hydrodynamic evolution, provide an average $\langle dS/d\eta_s \rangle = 37.59$ for minimum-bias pp collisions, in good agreement with the estimate found in Ref. [23]. This translates into a final charged-particle multiplicity $dN_{\rm ch}/d\eta \approx 5.22$, to be compared with the experimental values $4.63^{+0.30}_{-0.19}$ and $5.74^{+0.15}_{-0.15}$ measured by ALICE [24] in nonsingle-diffractive proton-proton collisions at $\sqrt{s} = 2.76$ and 7 TeV. Besides verifying that the present initialization and hydrodynamic evolution lead to the correct average hadron multiplicity, in the right panel of Fig. 1 one can see that the charged-particle multiplicity-distribution itself, with its KNO scaling [25], is reasonably well-described. Thus, by selecting the 0–1% percentile of the initial $dN_{\rm ev}/dS_0$ distribution we also construct a sample of about 10^3 high-multiplicity events, with $\langle dS/d\eta_s \rangle = 187.53$. Although our purpose is not to perform a precision study of soft observables, these checks allowed us to validate the model of the fireball assumed to be produced in proton-proton collisions and in which the heavy quarks propagate and undergo hadronization.

The initial quark-antiquark pairs are generated with the POWHEG-BOX [26] tool, which simulates the hard event and—once interfaced with PYTHIA—the associated initial and final-state parton-shower and other nonperturbative effects like the intrinsic-k_T of the incoming partons. Here we focus on charm, for which more experimental data are available. In generating the hard events we set the charm mass to $m_c = 1.3$ GeV, employing the default factorization and renormalization scales. Both in the minimum-bias and high-multiplicity cases—each sample containing about 10^3 independent proton-proton collisions—we generate 10^7 $c\bar{c}$ pairs, which are distributed among the different pp events according to their initial $dS/d\eta_s$. The initial position of the pairs in the transverse plane is sampled according to the local entropy density $s_0(\vec{x}_\perp)$. Hence, even in the minimum-bias sample, the $c\bar{c}$ pairs tend to be concentrated in the hot-spots of the events with the largest $dS/d\eta_s$. This is the analogous of the so-called "pedestal effect" [27], i.e. the fact that hadronic collisions containing pairs of jets are characterized by a higher activity also outside the jet cones. As a result, when distributing the $c\bar{c}$ pairs among the different pp events of the minimum-bias sample, only about 5% of them are found at τ_0 in a fluid cell below the hadronization temperature $T_H = 155$ MeV; this fraction drops to 1% when considering the high-multiplicity sample. This explains why the same modifications of the heavy-flavor hadrochemistry supposed to be a distinctive feature of nuclear collisions are also observed in the pp case; the shorter lifetime of the fireball going from AA to pp collisions only affects the kinematic distributions of the hadrons arising from the recombination process, but not their integrated yields, which simply depend on the existence of a color-reservoir and not on its flow.

Starting from the longitudinal proper-time τ_0 we simulate the stochastic dynamics of charm quarks through the fireball. No preequilibrium evolution neither of the heavy quarks nor of the medium is considered. The heavy-quark propagation in the expanding QGP is described through the relativistic Langevin equation. The latter allows one to update the heavy-quark momentum during the time-step Δt in the local rest-frame (LRF) of the fluid,

$$\Delta\vec{p}/\Delta t = -\eta_D(p)\vec{p} + \vec{\xi}(t), \tag{3}$$

where $\vec{\xi}$ is a noise term responsible for the in-medium momentum broadening, specified by its temporal correlator $\langle \xi^i(\vec{p}_t)\xi^j(\vec{p}_{t'})\rangle = b^{ij}(\vec{p}_t)\delta_{tt'}/\Delta t$, with

$$b^{ij}(\vec{p}) \equiv \kappa_\parallel(p)\hat{p}^i\hat{p}^j + \kappa_\perp(p)(\delta^{ij} - \hat{p}^i\hat{p}^j). \tag{4}$$

In the above the transport coefficients $\kappa_{\parallel/\perp}$ quantify the average longitudinal/transverse squared-momentum exchange per unit time with the medium. For them we use results provided by weak-coupling [hard-thermal-loop (HTL)] and the most recent lattice-QCD (lQCD) calculations [28]. Once $\kappa_{\parallel/\perp}$ are known, the friction coefficient η_D is fixed by a generalized Einstein relation ensuring the approach to kinetic equilibrium. More details can be found in [7,8]. We can quantify the time spent by the heavy quarks in the fireball before hadronization. In our minimum-bias sample for the average longitudinal proper-time at which charm quarks hadronize we found $\langle\tau_H\rangle \approx 1.95$ fm/c, with a $\tau_H^{\max} \approx 4.25$ fm/c. In the 0–1% high-multiplicity sample we found $\langle\tau_H\rangle \approx 2.92$ fm/c, with a $\tau_H^{\max} \approx 4.79$ fm/c. The longer time spent in a fireball with larger pressure gradients will lead to a larger radial flow of charmed hadrons in high-multiplicity pp collisions.

We now briefly summarize the hadronization model employed in this paper, based on a *local* color neutralization mechanism discussed in detail in [9] and illustrated in Fig. 2. We assume that once a c quark reaches the hadronization hypersurface at $T_H = 155$ MeV it undergoes recombination with an opposite color charge—either a light antiquark or a diquark, both assumed to populate the fireball according to their thermal abundance—*from the same fluid cell*; long-range interactions are in fact screened and, furthermore, this choice leads to a minimization of the confining potential. Diquark masses are taken from PYTHIA 6.4 [29]. For simplicity, no γ_s fugacity factor is introduced to suppress strange quarks in low-multiplicity pp events, which in any case provide a minor contribution to charm production. Even in the minimum-bias sample, if one weights each proton-proton collision by the average number of produced $c\bar{c}$ pairs one gets $\langle dS/d\eta_s\rangle_{c\bar{c}} \approx 68.87$, corresponding to $dN_{\rm ch}/d\eta \approx 9.56$, a multiplicity at which the observed enhancement of strange-particle production is already substantial [30]. After selecting from a thermal distribution both the species and the momentum of the heavy-quark companion in the LRF of the fluid, a color-singlet cluster is constructed. Since the recombining partons belong to the same fluid cell, in the laboratory frame there is a strong correlation—referred to as space-momentum correlation (SMC)—between the heavy-quark position, its momentum and the one of its light companion. Hence recombination usually occurs between

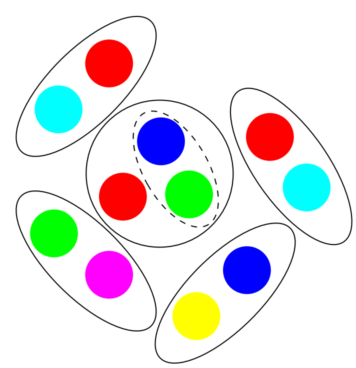

FIG. 2. A cartoon of our *local* color-neutralization mechanism via quark-antiquark or quark-diquark recombination of the closest opposite color charges.

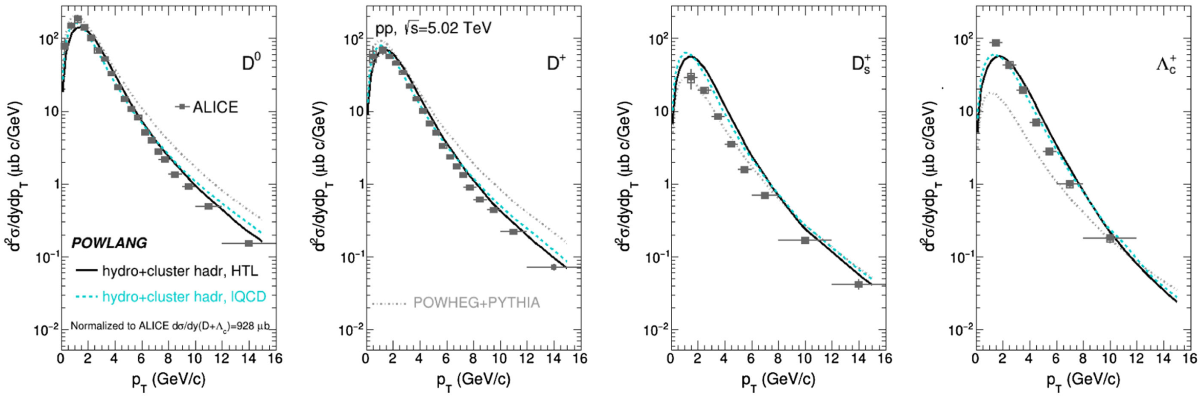

FIG. 3. Charmed hadron p_T-distributions in pp collisions at $\sqrt{s} = 5.02$ TeV normalized to the ALICE estimate for the $D + \Lambda_c^+$ cross section. Results obtained with POWHEG-BOX standalone and supplemented with an in-medium transport + hadronization stage with HTL and lattice-QCD transport coefficients are compared to ALICE data [1,33].

quite collinear particles in the laboratory frame: this favors the formation of low invariant-mass clusters. As in the HERWIG event generator [31], light clusters (below an invariant mass around 4 GeV) undergo a two-body decay, producing a charmed hadron accompanied by a pion (65% of cases) or a photon, if only this channel is kinematically open or if it is predicted by the PDG for resonances around that invariant mass. The decay is isotropic in the cluster rest frame, but due to SMC the cluster is boosted along the direction of expansion of the fireball. Hence, this local recombination mechanism efficiently transfers the collective flow of the fireball to the final charmed hadrons. Concerning higher invariant-mass clusters, these are treated as strings and hadronized with PYTHIA 6.4 [29], which simulates their fragmentation into hadrons. The present hadronization mechanism is quite schematic, but it has three main virtues; at variance with a pure $2/3 \to 1$ coalescence process, thanks to its $2 \to 1^* \to N$ dynamics, it conserves four-momentum exactly, it accounts for the enhanced baryon production via recombination with diquarks, and it includes (by construction) SMC which has a deep impact on the momentum and angular distributions of the final particles [9].

Results. Our predictions for the charmed-hadron p_T-differential cross sections in proton-proton collisions are shown in Fig. 3 for D^0, D^+ and D_s^+ mesons and for Λ_c^+ baryons. Indeed, current pQCD predictions tend to underestimate the $c\bar{c}$ production cross section in hadronic collisions [32]. Since we are mainly interested into the relative yields of the various particles and on the shape of their momentum distributions, we rescale the p_T-spectra of the different hadrons by a common normalization given by the experimental $D + \Lambda_c^+$ production cross section measured by ALICE [32]. In the figure we display the results obtained with POWHEG-BOX standalone—in which, besides the parton shower, also the hadronization stage is simulated with PYTHIA 6.4—and the ones in which the formation of a small fireball is assumed. One can see that POWHEG-BOX standalone underpredicts the Λ_c^+ production and misses the slope of the spectra. On the other hand,

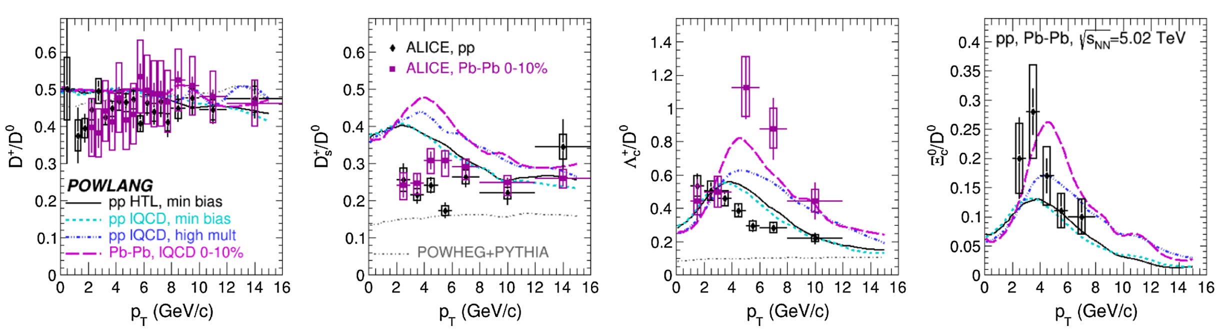

FIG. 4. Charmed-hadron yield ratios as a function of p_T for different colliding systems at $\sqrt{s_{\rm NN}} = 5.02$ TeV. Predictions including in-medium transport + hadronization in minimum-bias and high-multiplicity pp collisions and in central Pb-Pb collisions (see legend) are compared to ALICE data [1,2,33–35]. The enhanced baryon-to-meson ratio and the shift of its peak in denser systems is qualitatively well-reproduced. Also shown are the pp predictions of POWHEG + PYTHIA standalone, with no medium effects, which undershoots charmed-baryon production.

including heavy quark rescattering and hadronization in the fireball leads to a better description of the experimental data, with an enhanced Λ_c^+ production and steeper p_T spectra.

In Fig. 4 we plot, as a function of p_T, various charmed-hadron yield ratios. One can appreciate the enhanced D_s^+ and charmed-baryon production with respect to expectations based on vacuum fragmentation; this experimental observation is reproduced by our model (which slightly overestimates D_s^+ production). The most striking feature of the data, qualitatively described by our model, is the peak in the baryon/meson ratio for $p_T \approx 3$–5 GeV/c arising from the radial flow of light diquarks. The peak moves to higher values of p_T going from minimum-bias to high-multiplicity pp and, eventually, to central Pb-Pb collisions, consistently with the higher average radial velocity of the fluid cells where heavy-quark hadronization occurs ($\langle u_\perp \rangle_{\rm pp}^{\rm mb} \approx 0.33$–$0.34$, $\langle u_\perp \rangle_{\rm pp}^{\rm hm} \approx 0.53$–$0.54$ and $\langle u_\perp \rangle_{\rm PbPb}^{0-10\%} \approx 0.65$–$0.67$, depending on the choice of the transport coefficients). At very high p_T, one recovers the $\Lambda_c^+/D^0 \approx 0.1$ result typical of vacuum fragmentation. In fact, in this kinematic domain, charmed hadrons mainly come from the decay of high invariant-mass strings, which fragment as in vacuum.

Our study is also relevant to correctly quantify medium effects in heavy-ion collisions, where the pp benchmark enters in defining the nuclear modification factor $R_{\rm AA}(p_T) \propto (dN/dp_T)_{\rm AA}/(dN/dp_T)_{\rm pp}$. As one can see in Fig. 5, the inclusion of medium effects in pp collisions allows one to correctly reproduce the location and magnitude of the radial-flow peak (i.e. the reshuffling of the particle momenta, from low to moderate p_T) and to obtain a species dependence of the results with the same qualitative trend of the experimental data.

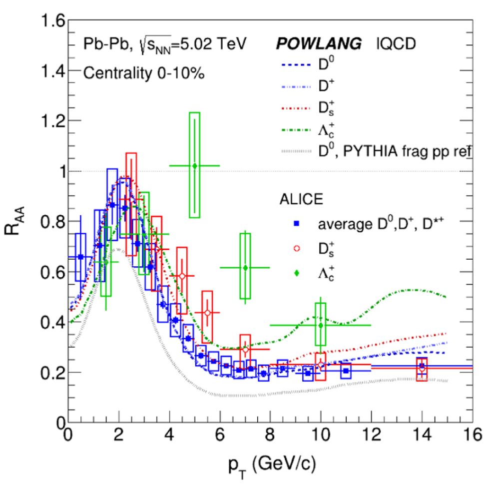

FIG. 5. Nuclear modification factor of charmed hadrons. Theory curves, obtained with lQCD transport coefficients, includes in-medium transport + hadronization in the minimum-bias pp benchmark and are compared to ALICE data [34,35]. Also shown is the D^0 result with no medium effect in the pp benchmark.

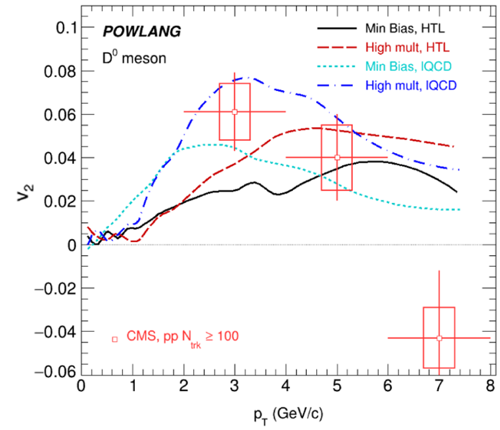

FIG. 6. D^0-meson elliptic-flow coefficient in minimum-bias and high-multiplicity pp collisions at $\sqrt{s} = 5.02$ TeV. Our predictions are compared to CMS results for high-multiplicity pp collisions at $\sqrt{s} = 13$ TeV [37].

Finally, it is interesting to study the response of the charmed-hadron azimuthal distributions to the initial deformation of the fireball produced in pp collisions, quantified on an EBE basis, according to Ref. [36], via the eccentricity ϵ_2 and the orientation ψ_2 of the minor axis of the approximate elliptic distribution of deposited entropy. For the former one ges $\langle \epsilon_2 \rangle \approx 0.31$, quite independent from the event activity. One then evaluates the charmed-hadron elliptic-flow coefficient $v_2 \equiv \langle \cos[2(\phi - \psi_2)] \rangle$, plotted in Fig. 6 for minimum-bias and high-multiplicity events and compared to CMS data for high-multiplicity pp collisions [37]. An important fraction of the v_2 is acquired at hadronization and the larger value obtained in high-multiplicity events has to be attributed not to a different initial deformation of the fireball, but to its longer lifetime.

Conclusions and perspectives. The assumption of the formation of a small deconfined fireball also in pp collisions, affecting the propagation and the hadronization of charm quarks, leads to a consistent picture of several experimental observations involving heavy-flavor hadrons: the slope of their momentum distributions, the p_T-dependent enhancement of the baryon-to-meson ratios, the nuclear-modification factor of their p_T distributions and the nonvanishing elliptic-flow coefficient. A more systematic study—exploring for instance the sensitivity of our results to the effective light quark and diquark masses, different implementations of subnucleonic fluctuations and inclusion of preequilibrium dynamics—is surely welcome, but we believe that our major findings will not change, being simply based on a local parton-recombination process occurring at a temperature around the confinement crossover within a fluid-cell undergoing a collective flow. What happens in the prehydrodynamic stage can only affect the collective velocity of the fireball, but cannot significantly alter the above picture. Our results provide independent, strong indications that the collective phenomena observed in small systems have the same origin as those measured in heavy-ion collisions. So far this was only inferred from the study of soft observables, i.e. from light hadrons emitted in the late stage of the fireball evolution. Having shown that the formation of a small QGP droplet in proton-proton collisions also affects the production of hard particles like heavy-flavor hadrons represents an important phenomenological and conceptual achievement, which, furthermore, entails reconsidering the universality of hadronization.

As a next step, we plan to extend our study to proton-nucleus collisions and to the hadronization of bottom quarks, so to provide a unified picture of heavy-flavor production across all colliding systems.

Acknowledgments. D. P. received funding from the European Union's Horizon 2020 research and innovation program under the Marie Sklodowska-Curie Grant Agreement No. 754496.

[1] S. Acharya *et al.* (ALICE Collaboration), Phys. Rev. Lett. **127**, 202301 (2021).
[2] S. Acharya *et al.* (ALICE Collaboration), J. High Energy Phys. 10 (2021) 159.
[3] V. Minissale, S. Plumari, and V. Greco, Phys. Lett. B **821**, 136622 (2021).
[4] J. Song, H.-h. Li, and F.-l. Shao, Eur. Phys. J. C **78**, 344 (2018).
[5] M. He and R. Rapp, Phys. Lett. B **795**, 117 (2019).
[6] J. R. Christiansen and P. Z. Skands, J. High Energy Phys. 08 (2015) 003.
[7] W. M. Alberico, A. Beraudo, A. De Pace, A. Molinari, M. Monteno, M. Nardi, F. Prino, and M. Sitta, Eur. Phys. J. C **73**, 2481 (2013).
[8] A. Beraudo, A. De Pace, M. Monteno, M. Nardi, and F. Prino, J. High Energy Phys. 02 (2018) 043.
[9] A. Beraudo, A. De Pace, M. Monteno, M. Nardi, and F. Prino, Eur. Phys. J. C **82**, 607 (2022).
[10] U. Heinz and R. Snellings, Annu. Rev. Nucl. Part. Sci. **63**, 123 (2013).
[11] C. Gale, S. Jeon, and B. Schenke, Int. J. Mod. Phys. A **28**, 1340011 (2013).
[12] R. D. Weller and P. Romatschke, Phys. Lett. B **774**, 351 (2017).
[13] J. S. Moreland, J. E. Bernhard, and S. A. Bass, Phys. Rev. C **92**, 011901 (2015).
[14] B. Schenke, P. Tribedy, and R. Venugopalan, Phys. Rev. Lett. **108**, 252301 (2012).
[15] All these parameters were calibrated using Bayesian inference [16], but we have had to modify k from 0.19 to 0.3 in order to describe the KNO scaling in pp collisions measured in experiments, see right panel of Fig. 1.
[16] J. S. Moreland, J. E. Bernhard, and S. A. Bass, Phys. Rev. C **101**, 024911 (2020).
[17] B. Schenke, S. Jeon, and C. Gale, Phys. Rev. C **82**, 014903 (2010).
[18] B. Schenke, S. Jeon, and C. Gale, Phys. Rev. Lett. **106**, 042301 (2011).
[19] J.-F. Paquet, C. Shen, G. S. Denicol, M. Luzum, B. Schenke, S. Jeon, and C. Gale, Phys. Rev. C **93**, 044906 (2016).
[20] A. Bazavov *et al.* (HotQCD Collaboration), Phys. Rev. D **90**, 094503 (2014).
[21] G. S. Denicol, T. Kodama, T. Koide, and P. Mota, Phys. Rev. C **80**, 064901 (2009).
[22] F. Cooper and G. Frye, Phys. Rev. D **10**, 186 (1974).
[23] P. Hanus, A. Mazeliauskas, and K. Reygers, Phys. Rev. C **100**, 064903 (2019).
[24] J. Adam *et al.* (ALICE Collaboration), Eur. Phys. J. C **77**, 33 (2017).
[25] Z. Koba, H. B. Nielsen, and P. Olesen, Nucl. Phys. **B40**, 317 (1972).
[26] S. Alioli, P. Nason, C. Oleari, and E. Re, J. High Energy Phys. 06 (2010) 043.
[27] G. Arnison *et al.* (UA1 Collaboration), Phys. Lett. B **132**, 214 (1983).
[28] L. Altenkort, O. Kaczmarek, R. Larsen, S. Mukherjee, P. Petreczky, H.-T. Shu, and S. Stendebach, Phys. Rev. Lett. **130**, 231902 (2023).
[29] T. Sjostrand, S. Mrenna, and P. Z. Skands, J. High Energy Phys. 05 (2006) 026.
[30] J. Adam *et al.* (ALICE Collaboration), Nat. Phys. **13**, 535 (2017).
[31] B. R. Webber, Nucl. Phys. **B238**, 492 (1984).
[32] S. Acharya *et al.* (ALICE Collaboration), Phys. Rev. D **105**, L011103 (2022).
[33] S. Acharya *et al.* (ALICE Collaboration), J. High Energy Phys. 05 (2021) 220.
[34] S. Acharya *et al.* (ALICE Collaboration), J. High Energy Phys. 01 (2022) 174.
[35] S. Acharya *et al.* (ALICE Collaboration), Phys. Lett. B **839**, 137796 (2023).
[36] Z. Qiu and U. W. Heinz, Phys. Rev. C **84**, 024911 (2011).
[37] A. M. Sirunyan *et al.* (CMS Collaboration), Phys. Lett. B **813**, 136036 (2021).